HHS Public Access

Author manuscript

FASEB J. Author manuscript; available in PMC 2025 January 17.

Published in final edited form as:

FASEB J. 2023 November ; 37(11): e23247. doi:10.1096/fj.202301417R.

Targeting sphingosine kinase 1 in p53KO thymic lymphoma

Fabiola N. Velazquez[1,2], **Jeffrey L. Stith**[1,2], **Leiqing Zhang**[1,2], **Amira M. Allam**[1,2], **John Haley**[3], **Lina M. Obeid**[1,2], **Ashley J. Snider**[1,2,4], **Yusuf A. Hannun**[1,2]

[1]Department of Medicine, Stony Brook University, Stony Brook, New York, USA

[2]Cancer Center, Stony Brook University, Stony Brook, New York, USA

[3]Biological Mass Spectrometry Center, Stony Brook Medicine, Stony Brook University, Stony Brook, New York, USA

[4]School of Nutritional Sciences and Wellness, College of Agriculture and Life Sciences, and University of Arizona Cancer Center, University of Arizona, Tucson, Arizona, USA

Abstract

Sphingosine kinase 1 (SK1) is a key sphingolipid enzyme that is upregulated in several types of cancer, including lymphoma which is a heterogenous group of malignancies. Treatment for lymphoma has improved significantly by the introduction of new therapies; however, subtypes with tumor protein P53 (p53) mutations or deletion have poor prognosis, making it critical to explore new therapeutic strategies in this context. SK1 has been proposed as a therapeutic target in different types of cancer; however, the effect of targeting SK1 in cancers with p53 deletion has not been evaluated yet. Previous work from our group suggests that loss of SK1 is a key event in mediating the tumor suppressive effect of p53. Employing both genetic and pharmacological approaches to inhibit SK1 function in *Trp53*KO mice, we show that targeting SK1 decreases tumor growth of established p53KO thymic lymphoma. Inducible deletion of *Sphk1* or its pharmacological inhibition drive increased cell death in tumors which is accompanied by selective accumulation of sphingosine levels. These results demonstrate the relevance of SK1 in the growth and maintenance of lymphoma in the absence of p53 function, positioning this enzyme as a potential therapeutic target for the treatment of tumors that lack functional p53.

Keywords

apoptosis; lymphoma; mice; p53; sphingosine; sphingosine kinase 1

Correspondence: Fabiola N. Velazquez, The MART Building, Stony Brook University, Stony Brook, NY 11794, USA. fabiola.velazquez@stonybrookmedicine.edu.

AUTHOR CONTRIBUTIONS

Lina M. Obeid, Fabiola N. Velazquez, Ashley J. Snider and Yusuf A. Hannun conceived the project and designed the experiments. Ashley J. Snider and Fabiola N. Velazquez developed the methodology. Fabiola N. Velazquez and Jeffrey L. Stith performed the experiments and aquired the data. Leiqing Zhang and Amira M. Allam provided technical support for animal studies. John Haley performed the pharmacokinetic study. Fabiola N. Velazquez, Jeffrey L. Stith, Ashley J. Snider and Yusuf A. Hannun interpreted and analyzed the data. Fabiola N. Velazquez wrote the manuscript. Jeffrey L. Stith, Ashley J. Snider, John Haley and Yusuf A. Hannun edited the manuscript. Ashley J. Snider and Yusuf A. Hannun supervised the study.

DISCLOSURES

The authors declare no potential conflicts of interest.

1 | INTRODUCTION

The bioactive lipids, ceramide (Cer), sphingosine (Sph) and sphingosine-1-phosphate (S1P), have key roles in the regulation of cancer cell signaling by controlling tumor suppression or survival.[1] Sphingosine kinase 1 (SK1), one of two SK proteins, is a highly regulated enzyme that produces the bioactive sphingolipid S1P, driving Sph and Cer to the only exit point of the sphingolipid pathway. SK1 has a central role in tumor biology[2] and has emerged as a possible therapeutic target in different types of cancers.[3] Upregulation of SK1 expression has been shown in different tumoral conditions[4] including hematological malignancies such as acute lymphoblastic leukemia,[5] erythroleukemia,[6] diffuse large B cell lymphoma (DLBCL)[7] as well as other subtypes of Non-Hodgkin Lymphoma.[8] Lymphoma is comprised of a heterogenous group of neoplasms that differ in their aggressiveness and response to treatment.[9] The emergence of immunotherapy and novel chemotherapy protocols have driven an improvement in the treatment of human lymphomas; however, specific subtypes of lymphoma such as peripheral T cell lymphomas (PTCL) still have low survival,[10] and relapse after treatment is a major concern that occurs in approximately 25%–30% of patients with DLBCL.[11,12]

Studies have started to uncover the importance of SK1 in lymphoma and the mechanisms by which it may regulate progression and growth of tumors. In DLBCL, *SPHK1* mRNA expression has been associated with tumor angiogenesis.[7] In Cutaneous T cell lymphoma, metabolism of Sph and S1P appears among the three most significantly altered pathways between control and tumor samples in mice,[13] suggesting an important role for sphingolipid enzymes involved in the regulation of these lipid species. Recent work has determined that natural killer T-cell activation could be modulated by SK1 expression in mantle T cell lymphoma[14]; however, the importance of this mechanism in tumor growth in vivo was not evaluated. Importantly, recent evidence proposes that S1P signaling contributes to the agressiveness of obesity-associated lymphoma[15] through the regulation of tumor cell survival and anti-tumor immune response. These findings support the continued evaluation of therapeutic strategies attributed to SK1 in different subtypes of lymphoma with the aim of controlling tumor growth.

Further linking SK1 and lymphoma is its association with the tumor suppressor protein p53. P53 has been proposed to modulate sphingolipid metabolism,[16,17] including the regulation of SK1 expression and stability. Previous findings demonstrated that SK1 is degraded in a p53 dependent manner in a human T lymphoblastic cell line (Molt4).[18] Following DNA damaging stressors, p53 induces the release of lysosomal and mitochondrial proteases that contributes to SK1 down-regulation. This mechanism is abrogated when p53 is degraded as a consequence of the expression of the papilloma protein E6 (Molt4E6 cells), suggesting a higher stability of SK1 protein in the absence of p53. Subsequently, we showed that the combined knockout (KO) of *Sphk1* and *Trp53* in mice prevents the development of thymic lymphoma and reduces the development of other tumors.[19] These findings raise the question whether SK1 could be used as a target for the treatment of established tumors with p53 dysfunction as opposed to preventing emergence of the thymic lymphoma. Indeed, it has been suggested that targeting SK1 can not only be detrimental for different tumoral cell lines

but also can control tumor growth in vivo using different mouse models.[2,20,21] However, the effect of this approach in tumors deficient in p53 has not been evaluated yet.

P53 is one of the most important tumor suppressor proteins, involved in a diverse set of cellular functions[22] with more than 50% of human cancers displaying a disruption of normal p53 function.[23] According to the TP53 database, hematological malignancies account for 5.91% of cancers with p53 mutations and its prevalence in tumors located in lymph nodes is approximately 19.34%. Although other tumor types show higher prevalence of p53 mutations, differences in prevalence are observed between subtypes of lymphoma, and survival of lymphoma patients is negatively affected by p53 mutations.[24,25] Even though most of the lymphomas are curable, the existence of specific subtypes, where the lack of p53 function is related with poor prognosis and survival, makes it important to continue evaluating alternative therapies in this specific context.

Owing to the fact that SK1 protein is more stable in the absence of p53, we hypothesized that the loss or inhibition of SK1 in tumors deficient in p53 may result in tumor regression of established thymic lymphomas. To test this hypothesis, we used *Trp53KO* mice that in addition harbor an inducible KO for *Sphk1*. In this mouse model, the results showed that the deletion of *Sphk1* decreased thymic lymphoma growth. Moreover, treatment of *Trp53KO* mice with the SK1 inhibitor PF543 reduced progression of thymic lymphoma growth. Increased cell death was observed in both genetic and pharmacological mouse models after targeting SK1. Additionally, analysis of lipid levels in tumor samples showed a specific increase in Sph, a lipid that results in apoptosis of p53KO thymic lymphoma cells in culture. This is the first study that demonstrates an important role for SK1 in the growth of thymic lymphomas with p53 malfunction, pointing to this enzyme as a possible novel target in p53 null cancers.

2 | MATERIALS AND METHODS

2.1 | Animals

Sphk1$^{fl/fl}$ mice were described previously.[26] *Sphk1*$^{fl/fl}$ were crossed with *Mx1Cre*$^{+}$ mice (C57BL6, Jackson Laboratory, Bar Harbor, ME, USA) to generate hematopoietic-specific inducible KO mice for *Sphk1* (*Sphk1*$^{fl/fl}$ *Mx1Cre*$^{+}$ mice). *Sphk1*$^{+/+}$ *Mx1Cre*$^{+}$ mice were used as controls. Mice used for experiments were > 8 weeks old. By breeding *Sphk1*$^{fl/fl}$ *Mx1Cre*$^{+}$ and *Trp53*$^{+/-}$ mice (C57BL/6, Jackson Laboratory), *Trp53*KO *Sphk1*$^{fl/fl}$ *Mx1Cre*$^{+}$ mice were obtained. *Trp53*KO *Sphk1*$^{+/+}$ *Mx1Cre*$^{+}$ were used as controls. Due to the decreased survival of *Trp53*KO female mice, only male mice were used for thymic lymphoma evaluation. *Trp53*KO mice that in addition to thymic lymphoma developed other types of tumors (sarcoma, osteosarcoma) were not used in these studies.

Genotype analysis was performed using PCR. All animal procedures were approved by the Northport Veterans Affairs Medical Center and Stony Brook University Institutional Animal Care and Use Committees. These approvals are based on U.S. National Institutes of Health and American Veterinary Medical Association guidelines.

2.2 | *Sphk1* deletion

Polyinosinic-polycytidylic acid (pIpC) (Invivogen, San Diego, CA, USA) was prepared in sterile endotoxin-free physiological water (NaCl 0.9%) at a concentration of 2 μg/μL. Mice were treated with 150 μL of pIpC solution by intraperitoneal (IP) injection, three times at three-day intervals.

2.3 | In vivo PF543 treatment

1% Hydroxypropyl Methyl Cellulose (HPMC) dissolved in PBS was used as a vehicle to prepare a suspension of PF543 (2.5 mg/mL). For pharmacodynamic evaluation of PF543, wildtype (WT) mice were administered a dose of 10 mg/kg of body weight by IP injection twice a day (morning/afternoon) for 20 days. *Trp53*KO mice that developed tumors were treated with PF543 for 10 days with a dose of 10 mg/kg of body weight (two IP injection per day).

2.4 | Blood counts

Whole blood was collected in EDTA tubes and analyzed on a Veterinary Hematology Analyzer (Drew Scientific Mascot HemaVet 950FS).

2.5 | Pharmacokinetic (PK) evaluation of PF543 in WT mice

PF543 was characterized by kinetic and equilibrium solubility, cell permeability (PAMPA), mouse hepatic microsome stability, IV/PO/IP pharmacokinetics, stability in mouse plasma and blood, inhibition of human cytochrome P450s, and mouse plasma binding. For mouse PK compound was formulated in 1% HPMC and dosed IP.

2.6 | Ultrasound monitor

*Trp53*KO, *Trp53*KO *Sphk1*$^{+/+}$ *Mx1Cre*$^{+}$ and *Trp53*KO *Sphk1*$^{fl/fl}$ *Mx1Cre*$^{+}$ mice were monitored by ultrasound imaging starting at ~3.5 months of age to detect development of thymic lymphoma. Animals were monitored weekly by ultrasound imaging using the Vevo 3100 Imaging System (FUJIFILM VisualSonics, Toronto, ON, Canada). When tumors reached 100–150 mm^3 in size, mice from the inducible model were injected with pIpC while mice for the pharmacological model were treated with PF543. To follow the response in vivo, tumors were imaged every three days by ultrasound and tumor volume was calculated (Volume = [Length × Width × Height] × π/6). Mice were euthanized at day 20 after the first pIpC injection (inducible model) or at day 10 after the first PF543 injection (pharmacological model). Tumor samples were collected and snap frozen in liquid nitrogen before being stored at −80°C until further processing and blood was collected for lipidomic analysis.

2.7 | Tissue homogenization

Tumor samples stored at −80°C were transferred to eppendorf tubes with screw caps containing glass beads and minced with dissecting scissors in 300 μL of RIPA lysis buffer (Santa Cruz Biotechnology, Dallas, TX, USA) for protein extraction, in 300 μL of RNA lysis buffer (PuroLink RNA RNA Mini Kit, Thermo Fisher Scientific, Danvers, MA, USA) containing 1% β-mercaptoethanol for RNA extraction, or in 500 μL of cell

extraction mixture (2:3 70%Isopropanol:Ethanol) for sphingolipid analysis. Tumor samples were homogenized using the FastPrep-24 lysis system (MP Biomedicals, Santa Ana, CA, USA). Samples for protein analysis were centrifuged at 10 000*g* for 10 min and kept at −80°C until further analysis. Samples for RNA extraction were processed following the manufacturer's protocol. Samples for lipid analysis were spun down, supernatant transferred to 15 mL falcon tubes and cell extraction mixture added to 2 mL of final volume. Samples for sphingolipid analysis were kept at −80°C until lipid extraction.

2.8 | qPCR analysis

Cells were collected by centrifugation at 800*g* for 5 min, washed one time in cold PBS, and then RNA was extracted following the manufacturer's protocol (PuroLink RNA RNA Mini Kit, Thermo Fisher Scientific). For both culture cell samples and tissue samples, cDNA was synthesized from 1.0 μg of RNA using SuperScript™ III First-Strand Synthesis SuperMix for qRT-PCR (Invitrogen, cat#11752250) according to the manufacturer's instructions. Real-time PCR was performed using Taqman assays on an Applied Biosystems 7500 RT-PCR System (Foster City, CA, USA). Threshold cycle values for target genes were normalized to the reference gene to determine mean normalized expression using the ΔΔCt method. Actin was used as a reference gene in all cases. Taqman assays were purchased from Thermo Fisher Scientific: Mouse SPHK1: Mm00448841_g1, Mouse SPHK2: Mm00445021_m1, mouse Actin: Mm00607939_s1.

2.9 | Western Blot

Primary antibodies used for Western blot included SK1 (1:1000, Cat #12071, Cell Signaling Technology), SK2 (1:1000, ab37977, Abcam), Parp1 (1:2000, Cat#9542, Cell Signaling Technology), cleaved caspase 3 (1:1000, Cat#9661, Cell Signaling Technology), caspase 8 (1:1000, Cat#4790, Cell Signaling Technology), caspase 7 (1:1000, Cat#12827, Cell Signaling Technology), caspase 9 (1:1000, Cat#95020, Cell Signaling Technology), p16 (1:1000, ab211542, Abcam), p21 (1:1000, sc-6246, Santa Cruz Biotechnology), Beta-Actin (1:25000, Cat. #A5441, Sigma Aldrich). After incubation with the appropriate secondary antibody, signal was detected using enhanced chemiluminescence or Supersignal West Dura Extended Duration Substrate (Life Technologies, Carlsbad, CA, USA) according to the manufacturer's instructions.

2.10 | Immunohistochemistry

Tumor samples were processed as described in Espaillat et al.[27] Slides were incubated overnight with anti-cleaved caspase-3 antibody (1:200, Cat#9661, Cell Signaling Technology) at 4°C. After incubation with biotinylated anti-rabbit antibody (Vector Laboratories, Burlingame, CA, USA), slides were developed with DAB/H2O2 (Thermo Scientific, Hudson, NH, USA), and counterstained with hematoxylin. Microscopy was performed using a Zeiss Axio Imager M2 (Jena, Germany) microscope. The number of positive cells for cleaved caspase 3 was determined by quantification of ten fields (20× magnification) per sample and the results expressed as the number of cleaved caspase 3 positive cells/mm^2.

2.11 | LC–MS/MS sphingolipid analysis

Cells were collected by centrifugation at 800*g* for 5 min. Then, cells were washed one time in cold PBS, centrifuged at 800*g* for 5 min, and cellular pellet resuspended in 2 mL of cell extraction mix (2:3 70%Isopropanol:Ethanol). Samples were kept at −80°C until lipid extraction.

Whole blood was mixed with 2 mL RPMI and then directly lysed with 2 mL media extraction mixture (15:85 isopropanol/ethyl acetate).

To perform sphingolipid quantification, samples from cell culture, tissue, or whole blood were spiked with the corresponding internal standards (50 pmol), and extracts were then analyzed by the Lipidomic Core Facility at Stony Brook University Medical Center, as described previously.[28] Lipid levels were normalized to total inorganic phosphate (for tissue and cell culture) or to volume (for whole blood).

2.12 | Cell culture and reagents

Human T lymphoblastic cell lines were grown in RPMI 1640 supplemented with 10% FBS (Fetal Bovine Serum), 100 units/mL penicillin and 100 μg/mL streptomycin. Molt4-LXSN (MOLT4) and Molt4E6 were previously described.[29]

To generate Jurkat gRNA V2, BakA and BakB cells, HEK293T cells were transfected with 2 μg plasmids containing 250 ng of pCMV-VSVG, 750 ng of pCMV-dR8.2 and 1 μg of pLenti CRISPR/Cas9/sgRNA. Two different synthetic guide RNA targeting Bak (BakA and BakB) were used. Supernatants were collected at 48 h post-transfection and used for infection of Jurkat cells. Transduced cells were selected by treatment with Puromycin 1 μM for 48 h.

The mouse *Trp53*KO thymic lymphoma cell line was generated as described[30] and cultured in 45%IMDM (Corning), 45%DMEM (Corning), 10%FBS (Gibco), 100 units/mL penicillin, 100 μg/mL streptomycin, 4 mM L-Glutamine and 25 μM 2-mercaptoethanol.

Primary WT lymphocytes were isolated from thymus of 8 weeks of age C57/B6 male mice as described.[31] WT lymphocytes were cultured in RPMI supplemented with 10% FBS, 2 mM L-glutamine, 0.01 mM 2-Mercaptoethanol, penicillin/streptomycin and 50 U/mL of Mouse IL-2.

Cells were evaluated for Mycoplasma contamination (Lonza Cat# #: LT07–710, MycoAlert PLUS Mycoplasma Detection Kit) before using them for analytical purposes.

Doxorubicin (Sigma Aldrich) and PF543 (Calbiochem) for cell culture treatment were dissolved in DMSO. D and L-*erythro*-Sph (Cayman Chemical) was dissolved in methanol.

2.13 | Cell counting

Cell suspension samples were diluted (1:1 dilution) in 0.4% trypan blue solution (ThermoFisher Scientific). Neubauer chambers were loaded with the stained cell suspension, and cells (non-viable (blue) and viable (unstained)) were counted under the microscope.

For the proliferation assay, the number of viable cells over time was counted. For the cell death assay, the percentage of trypan blue positive cells over the total number of cells (at a specific time point) was plotted.

2.14 | Viability assay

Viability of mouse *Trp53*KO thymic lymphoma cells was measured by CCK-8 assay (cat#96992, Sigma Aldrich) according to the manufacturer's instructions.

Viability for mouse WT lymphocytes was measured by MMT assay as described.[32] Cells were incubated with MTT 1 mg/mL during 2 h and then cells lysed in 10% SDS + 0.01 N HCl solution.

2.15 | Flow cytometry

*Trp53*KO lymphoma cells were washed twice in 1X PBS and resuspended in FACS buffer (1%BSA, 1 mM EDTA, 0.5% sodium azide in 1X PBS) at a concentration of 1×10^6 cells/100 μL. Cell suspensions were stained on ice in the dark for 30 min with the following fluorochrome-conjugated antibodies: anti-CD3-PE Dazzle 594 (1/100, Biolegend, cat#100245), anti-CD4-PE (1/100, Biolegend, cat#116005) and anti-CD8-BV650 (1/800, Biolegend, cat#100742). Live/Dead Fixable Scarlet (723) Cell Stain (ThermoFisher, cat# L34987) was used to exclude dead cells during analysis. Cells were analyzed using BD LSR-Fortessa Cell Analyzer.

2.16 | Statistical analysis

Statistical analyses were performed using GraphPad Prism (GraphPad Software). Data are presented as mean ± SEM and were analyzed by one-way ANOVA with a Dunn's Multiple Comparison Test or by unpaired Student's *t* test. $p < .05$ was considered statistically significant.

3 | RESULTS

3.1 | Generation of an inducible knockout model for *Sphk1*

Previous studies have shown that *Sphk1* deletion prevents the formation of thymic lymphoma in *Trp53*KO mice.[19] Additionally, results in cultured cells have determined a higher stability of SK1 protein in *Trp53*KO compared to *Trp53*WT condition (Figure S1).[18,33] However, the impact of targeting SK1 in established *Trp53*KO tumors in vivo has not been determined, and this is critical to evaluate if SK1 is required for maintenance (vs only in initiation) of thymic lymphomas. To evaluate this, the effect of *Sphk1* deletion in established *Trp53*KO thymic lymphoma was assessed. First, an inducible KO mouse for *Sphk1* (*Sphk1*$^{fl/fl}$ *Mx1Cre*$^{+}$ mice) in hematopoietic cells was generated (Figure 1A). Ten days post injections with pIpC (Figure 1B) *Sphk1* mRNA expression decreased more than 90% in thymus (Figure 1C), while *Sphk2* mRNA expression significantly increased (Figure 1D). Additionally, measurement of *Sphk* expression in bone marrow showed a decrease in *Sphk1* mRNA with no changes in *Sphk2* mRNA (Figure S2A). Although sphingolipid measurements in the thymus did not exhibit differences in Sph or S1P levels after *Sphk1* deletion (Figure S2B), circulating S1P significantly decreased (Figure 1E), indicating *Sphk1*

deletion in the hematopoietic system. These results suggest that Mx1 activation results in an efficient *Sphk1* deletion in the thymus of *Sphk1*$^{fl/fl}$ *Mx1Cre*$^{+}$ mice. Therefore, these mice can be used as an inducible KO model for *Sphk1*.

3.2 | *Sphk1* ablation in *Trp53*KO mice prevents progression of thymic lymphoma

To evaluate the effect of *Sphk1* deletion in *Trp53*KO thymic lymphoma, *Trp53*KO *Sphk1*$^{fl/fl}$ *Mx1Cre*$^{+}$ mice were generated. These mice have a very high incidence of lymphomas (~70%) by the age of 4.5 months.[34,35] The thymus is special in that, unlike most organs, it gradually atrophies and decreases in size and weight with age (thymic involution); therefore, a significant increase in the volume over time is taken as an indication of tumor initiation. Thymic lymphoma development was detected by ultrasound imaging, and when the size of the tumor reached a volume between 100–150 mm^3, *Sphk1* was deleted by IP injections with pIpC (Figure 2A). *Trp53*KO *Sphk1*$^{+/+}$ *Mx1Cre*$^{+}$ mice that received pIpC injections were used as controls since they retain WT *Sphk1* expression. Mice were euthanized after 20 days of pIpC treatment. Analysis of mRNA expression in the tumor revealed a significant decrease in *Sphk1* expression in *Trp53*KO *Sphk1*$^{fl/fl}$ *Mx1Cre*$^{+}$ mice (Figure 2B), with no significant changes in *Sphk2* mRNA (Figure S3A). Tumors in *Trp53*KO *Sphk1*$^{fl/fl}$ *Mx1Cre*$^{+}$ mice demonstrated significant growth inhibition when compared to *Trp53*KO *Sphk1*$^{+/+}$ *Mx1Cre*$^{+}$ mice (Figures 2C,E and S3B). Additionally, tumor weight was significantly decreased following *Sphk1* deletion (Figure 2D). These data suggest that deletion of *Sphk1* in established tumors decreased progression of thymic lymphoma growth in *Trp53*KO mice.

3.3 | *Sphk1* ablation results in selective increase in levels of Sph in *Trp53*KO thymic lymphoma

Previous work by our group determined that loss of p53, as well as the double KO of *Trp53* and *SphK1*, significantly altered sphingolipid levels in thymic lymphomas. Therefore, we examined the impact of *Sphk1* deletion on sphingolipid levels in our mouse model to begin to determine the potential role for these lipid mediators in inhibition of tumor growth. Analysis of sphingolipid levels in blood demonstrated no significant differences between *Trp53*KO *Sphk1*$^{fl/fl}$ *Mx1Cre*$^{+}$ and control mice (Figure 3A). In tumor tissues following *Sphk1* deletion, S1P and Cer levels remained unaltered; however, Sph levels significantly increased (Figure 3B). Taken together, the results suggest that increased in Sph levels in the tumor may mediate regression of thymic lymphomas in *Trp53*KO mice after *Sphk1* deletion.

3.4 | Pharmacological inhibition of SK1 controls thymic lymphoma growth in *Trp53*KO mice

We next set out to extend our findings in the inducible mouse model and define the effects of a potent and specific SK1 inhibitor (PF543)[36] on thymic lymphoma growth. First, thymic lymphoma cells from a tumor developed in a *Trp53*KO mouse were isolated and cultured in vitro. Analysis of surface markers confirmed the immature phenotype (CD3+ CD4+ CD8+) of isolated tumor cells (Figure S4A), in agreement with lymphomas developed in *Trp53*KO mouse.[35] Treatment of these cells with PF543 significantly decreased proliferation over time in low-serum medium (Figure 4A,B) and resulted in cell death, partially protected by the pan-caspase inhibitor ZVAD (Figure S4B). Measurement of SK activity by C17 labeling confirmed SK1 inhibition in *Trp53*KO thymic lymphoma cells after PF543 treatment (Figure

4C). Additionally, Sph and total Cer levels were significantly increased in *Trp53*KO thymic lymphoma cells treated with PF543 (Figure 4D), indicative of SK1 inhibition. Importantly, evaluation of PF543 on lymphocytes isolated from WT thymus did not affect cell viability over time (Figure S4C). These data demonstrate that inhibition of SK1 does not affect WT lymphocyte viability but decreases growth of tumor cells deficient in p53.

To determine the appropriate dosing regime in vivo we performed PK studies in WT mice (Table 1). PF543 is a potent compound for in vitro evaluation but is limited in vivo by high plasma protein binding (94% bound) and low IV Cmax. IP dosing was established at 25 and 50 mg/kg, while 100 mg/kg was not tolerated. These studies confirmed the short half-life of PF543 (~4 h), as was previously suggested,[37] indicating the need for repeat administration of the drug to evaluate its effect on tumor growth in mice. Administration of PF543 decreased S1P levels in blood (Figure 5A). Long-term administration of PF543 in WT mice did not significantly impact body weight (Figure 5B), liver (Figure 5C), or kidney function (Figure 5D). The PK studies demonstrated safety and efficacy of PF543 in vivo, and importantly, no decrease in the number of total white cells and lymphocytes in blood was observed after long-term treatment of WT mice with PF543 (Figure 5E). Therefore, BID IP dosing at 10 mg/kg for treatment of *Trp53*KO mice was established. Similar to the inducible deletion of *SphK1*, thymic lymphomas were detected by ultrasound imaging, and when the size of the tumor reached a volume between 100–150 mm^3, PF543 was administered (Figure 5F). Treatment with PF543 resulted in significant inhibition of tumor growth in *Trp53*KO mice compared to vehicle (Figures 5G and S3C). Taken together these data demonstrate the therapeutic potential for SK1 inhibition in *Trp53*KO thymic lymphoma.

3.5 | Sph induces apoptosis in lymphoma cells

Our in vivo and in vitro results suggest Sph may be mediating the effects of SK1 loss and/or inhibition. To gain a better understanding about the mechanism by which Sph reduces thymic lymphoma growth, we performed mechanistic cell-based studies in culture. Sph treatment caused cell death (Figure 6A) associated with activation of caspases (Figure 6B) in Molt4E6 cells. The effects of Sph were stereospecific as L-erythro-Sph (a non-natural Sph that is the mirror image of D-erythro-Sph) did not induce cell death or caspase activation. Additionally, inhibition of ceramide generation with FB1 did not protect from Sph-induced cell death (Figure 6D,E), but pre-treatment with the pan-caspase inhibitor ZVAD significantly inhibited Sph-induced cell death (Figure 6C,E). These results indicate a caspase- dependent cell death caused by Sph in a stereospecific manner and independent of Cer synthesis in Molt4E6 cells. Previous reports have described similar results in other cellular systems,[1,38] particularly pointing to a critical role of mitochondria in Sph-induced cell death. In line with these studies, knockdown of the Bcl2 pore forming protein Bak in Jurkat cells significantly protected against Sph-induced cell death (Figure 6F). These results show that in lymphoma cells lacking p53 wildtype function, Sph causes apoptosis through a mitochondrial pathway.

3.6 | Increased cell death after targeting SK1 in *Trp53*KO thymic lymphoma

Tumor samples after *Sphk1* deletion or pharmacological inhibition of SK1 were analyzed, to start elucidating the mechanism(s) by which targeting SK1 controls thymic lymphoma growth in vivo. Although induction of a senescence phenotype was previously observed as one of the mechanisms by which loss of *Sphk1* protected against thymic lymphoma development in *Trp53*KO mice,[19] p21 or p16 expression was not altered in tumor samples from *Trp53*KO *Sphk1*$^{fl/fl}$ *Mx1Cre*$^{+}$ mice (Figure S5). Similarly, proliferation was not altered in tumor samples from *Trp53*KO *Sphk1*$^{fl/fl}$ *Mx1Cre*$^{+}$ mice (data not shown). In contrast, deletion of *Sphk1* resulted in increased Parp1 and caspase 3 cleavage in tumor samples from *Trp53*KO *Sphk1*$^{fl/fl}$ *Mx1Cre*$^{+}$ mice (Figure 7A). Additionally, the number of cleaved caspase 3 positive cells was significantly higher in tumor samples from PF543 treated mice compared to vehicle treated mice (Figure 7B). These results suggest that targeting SK1 in *Trp53*KO thymic lymphoma results in an increase in apoptosis which could contribute to the control of tumor growth and progression.

4 | DISCUSSION

The higher stability of SK1 protein in the absence of p53 function and the role it plays in regulating cell survival render SK1 an attractive target for the treatment of tumors that lack p53. In the present work, the effect of targeting SK1 in p53 null lymphomas was evaluated for the first time using a *Trp53*KO mouse model that spontaneously develops thymic lymphoma. Using two different approaches, a genetic and a pharmacological model, we show that targeting SK1 prevented thymic lymphoma progression accompanied by an increase in apoptotic cell death and Sph levels.

An inducible KO mouse for *Sphk1* (*Sphk1*$^{fl/fl}$ *MxCre*$^{+}$ mice)[26] was used as a model where the *Sphk1* gene can be deleted in the thymus. In this mouse strain, deletion of *Sphk1* induced by pIpC treatment occurred not only in the thymus but also in cells from hematopoietic linage.[39] Analysis of sphingolipid species in the thymus after *Sphk1* deletion did not show differences compared to control mice; however, circulating S1P was significantly decreased, in agreement with the phenotype described for *Sphk1*KO mice.[40] The lack of differences in S1P and Sph levels in thymic tissue could be explained by compensation in the expression or activity of other sphingolipid enzymes, lipid phosphate phosphatase 3[41] and S1P lyase[42] which closely regulate S1P levels in thymus. Although these enzymes were not evaluated, *Sphk2* expression was significantly increased after *Sphk1* deletion (Figure 1D) suggesting a possible compensation in metabolic activity of SK1 in the thymus. *Sphk1*$^{fl/fl}$ *MxCre*$^{+}$ mice showed an efficient deletion of *Sphk1* in thymus; consequently, this strain can be used to evaluate the role of this enzyme in pathological conditions that involved this tissue.

*Trp53*KO mice have been extensively used to study, not only the role of p53 as a tumor suppressor in vivo,[43–45] but also its interconnection with different proteins that participate in critical signaling pathways during carcinogenesis.[46,47] Our previous study in *Trp53*KO mice demonstrated that *Sphk1* deletion resulted in a senescence phenotype in the thymus, and as a consequence, *Trp53*KO *Sphk1*KO mice were protected against thymic lymphoma development.[19] In this work, deletion of *Sphk1* in *Trp53*KO bearing

tumor mice (after appearance and establishment of the tumors) did not result in expression of senescence markers, instead it caused an increase in cell death. The differential response against *Sphk1* absence could be explained by the unique cellular contexts.[48] It is possible that SK1 plays a role in senescence of pre-neoplastic *Trp53*KO cells, but after the tumor develops, the presence of different genetic alterations that go along with *Trp53*KO lymphoma development[49] confers a different biological response against disturbances in this sphingolipid enzyme, as has been shown for other proteins.[50] Under a tumoral condition, *Sphk1* deletion reduces *Trp53*KO thymic lymphoma growth associated with an increased cell death, suggesting an important role for Sphk1 expression in the survival of *Trp53*KO lymphoma.

To identify sphingolipid changes linked to the control of thymic lymphoma growth after targeting SK1, analysis of sphingolipid species was conducted in both *Trp53*KO thymic lymphoma after *Sphk1* deletion and *Trp53*KO thymic lymphoma cells after SK1 activity inhibition. While analysis of cultured cells showed an increase in Sph and Cer levels, evaluation of tumor samples showed a specific accumulation in Sph. Several reports have documented the toxic effect of Sph in different cancer cell lines,[51,52] including lymphoma/leukemia cells.[53] In most of the cellular systems evaluated, Sph induces a mitochondrial dependent cell death,[54] but the specific Sph targets upstream of this effect are not well established and seem to be highly dependent on the system.[55] The importance of Sph on cell death may have been underestimated due to its rapid metabolism to Cer, the central hub of sphingolipid metabolism also associated with cell death and for which molecular targets have been better determined.[56] Using the Cer synthase inhibitor FB1, we demonstrated that Sph can induce cell death in *Trp53*KO thymic lymphoma cells independently of ceramide accumulation. Additionally, we showed a critical role for mitochondria and caspases activation in the cytotoxic effect of Sph in lymphoma cells. Few studies have shown the association between Sph accumulation and tumor control growth in mouse models.[57] Although in the sphingolipid field the association between increased Sph and cell death is not unusual, in this study we confirm a mitochondrial pathway of apoptosis triggered by Sph in lymphoma cells that lack p53 function. A better understanding about the Sph targets upstream of mitochondrial damage are needed with the aim to improve therapeutic strategies directed to sphingolipid metabolism.

To extend the results observed in *Sphk1*$^{fl/fl}$ *MxCre*$^{+}$ *Trp53*KO mice, a pharmacological model, where SK1 was inhibited in *Trp53*KO tumor bearing mice, was designed. Among the different inhibitors of SK1 available, PF543 is the most specific inhibitor described.[36] Murine models of hypertension,[58] inflammation,[59,60] lung injury[61] and renal fibrosis[62] have shown a biological effect for PF543. Although several studies have reported low anticancer potential for PF543 in different cancer cell lines, in this work, PF543 reduced survival of mouse *Trp53*KO lymphoma cells in culture. More importantly, treatment of *Trp53*KO mice that develops thymic lymphoma resulted in an increased cell death and controlled tumor growth, in agreement with what was observed in the genetic model. The main inconvenience related to the use of PF543 in vivo is its short half-life after IP administration in mice (T1/2 = ~4 h). Indeed, pharmacological inhibition of SK1 was not as effective as *Sphk1* deletion (genetic model) in controlling *Trp53*KO thymic lymphoma growth. These differences could be explained by the very short half-life of PF543 and the fact that SK1

is not inhibited during all the interval following each treatment. Molecular modifications have been applied to PF543 to improve its anticancer potential[63] or to extend its inhibitory capacity to additional sphingolipid enzymes[64]; however, these new compounds were used at higher concentrations than the original drug, which could reduce specificity. The short half-life of PF543 in mice raises the need to identify either new inhibitors or additional molecular modifications to increase PF543 stability in biological systems and improve its bioavailability in mouse models of tumor growth.

In summary, the results obtained in this study place SK1 as an important player in the maintenance and growth of *Trp53*KO lymphomas. We propose that targeting SK1 increases Sph in p53KO lymphoma resulting in a mitochondrial apoptotic cell death which contributes to the control of thymic lymphoma. It remains to be determined what specific molecular pathways contribute to the results observed at both the intracellular level within the tumor and the possible contribution by the tumor microenvironment where SK1 product has a critical role in cancer signaling.[65] Using *Sphk1*KO mice in allograft or bone marrow transplantation models, the extrinsic and intrinsic contribution of SK1 in *Trp53*KO lymphoma progression can start to be further elucidated. Determining these pathways will help to improve or develop new therapeutic approaches. Although the survival of lymphoma patients has significantly improved by the introduction of new therapies including monoclonal antibody and chimeric antigen receptor T-cells, the treatment of specific subtypes of lymphoma, such as PTCL and refractory and relapsed diseases remains challenging. Particularly the presence of p53 mutations exerts a negative impact on lymphoma progression and patient prognosis. It would be pertinent to start the evaluation of targeting SK1 in p53 mutant lymphomas.

Supplementary Material

Refer to Web version on PubMed Central for supplementary material.

ACKNOWLEDGMENTS

The authors would like to acknowledge Dr. Christopher J. Clarke and Janet J. Allopenna for the pLenti CRISPR/Cas9/sgRNA constructs used in this work. The authors would also like to acknowledge the Sphingolipid Animal Cancer Pathobiology Core for the mouse models used in these studies, the Stony Brook University Lipidomic Shared Resource Core for technical support with lipid analysis, the Research Histology Core Laboratory (Department of Pathology, Stony Brook Medicine) and the Flow Cytometry Research Core Facility (Clinical Immunology Laboratory, Stony Brook Hospital) for their technical and analytical support. This work was supported by National Cancer Institute Grant P01-CA097132 and by Institutional Research Grant 21-143-01-IRG from the American Cancer Society.

DATA AVAILABILITY STATEMENT

The data generated in this study are available within the article and its supplementary data files. Raw data supporting the findings of this study are available from the corresponding author upon request.

REFERENCES

1. Taha TA, Mullen TD, Obeid LM. A house divided: ceramide, sphingosine, and sphingosine-1-phosphate in programmed cell death. Biochim Biophys Acta. 2006;1758:2027–2036. [PubMed: 17161984]
2. Heffernan-Stroud LA, Obeid LM. Sphingosine kinase 1 in cancer. Adv Cancer Res. 2013;117:201–235. [PubMed: 23290781]
3. Wang X, Sun Y, Peng X, et al. The tumorigenic effect of sphingosine kinase 1 and its potential therapeutic target. Cancer Control. 2020;27:1073274820976664.
4. Johnson KR, Johnson KY, Crellin HG, et al. Immunohistochemical distribution of sphingosine kinase 1 in normal and tumor lung tissue. J Histochem Cytochem. 2005;53:1159–1166. [PubMed: 15923363]
5. Wallington-Beddoe CT, Xie V, Tong D, et al. Identification of sphingosine kinase 1 as a therapeutic target in B-lineage acute lymphoblastic leukaemia. Br J Haematol. 2019;184:443–447. [PubMed: 29359799]
6. Le Scolan E, Pchejetski D, Banno Y, et al. Overexpression of sphingosine kinase 1 is an oncogenic event in erythroleukemic progression. Blood. 2005;106:1808–1816. [PubMed: 15890687]
7. Lupino L, Perry T, Margielewska S, et al. Sphingosine-1-phosphate signalling drives an angiogenic transcriptional programme in diffuse large B cell lymphoma. Leukemia. 2019;33:2884–2897. [PubMed: 31097785]
8. Bayerl MG, Bruggeman RD, Conroy EJ, et al. Sphingosine kinase 1 protein and mRNA are overexpressed in non-Hodgkin lymphomas and are attractive targets for novel pharmacological interventions. Leuk Lymphoma. 2008;49:948–954. [PubMed: 18452097]
9. Singh R, Shaik S, Negi BS, et al. Non-Hodgkin's lymphoma: a review. J Family Med Prim Care. 2020;9:1834–1840. [PubMed: 32670927]
10. Federico M, Bellei M, Marcheselli L, et al. Peripheral T cell lymphoma, not otherwise specified (PTCL-NOS). A new prognostic model developed by the international T cell project Network. Br J Haematol. 2018;181:760–769. [PubMed: 29672827]
11. Odejide OO, Cronin AM, Davidoff AJ, LaCasce AS, Abel GA. Limited stage diffuse large B-cell lymphoma: comparative effectiveness of treatment strategies in a large cohort of elderly patients. Leuk Lymphoma. 2015;56:716–724. [PubMed: 24913508]
12. Nijland M, Boslooper K, van Imhoff G, et al. Relapse in stage I(E) diffuse large B-cell lymphoma. Hematol Oncol. 2018;36:416–421. [PubMed: 29083044]
13. Le Y, Shen X, Kang H, et al. Accelerated, untargeted metabolomics analysis of cutaneous T-cell lymphoma reveals metabolic shifts in plasma and tumor adjacent skins of xenograft mice. J Mass Spectrom. 2018;53:739. [PubMed: 30133995]
14. Lee MS, Sun W, Webb TJ. Sphingosine kinase blockade leads to increased natural killer T cell responses to mantle cell lymphoma. Cells. 2020;9:1030. [PubMed: 32326225]
15. Wang X, Guo W, Shi X, et al. S1PR1/S1PR3-YAP signaling and S1P-ALOX15 signaling contribute to an aggressive behavior in obesity-lymphoma. J Exp Clin Cancer Res. 2023;42:3. [PubMed: 36600310]
16. Jeffries KA, Krupenko NI. Ceramide signaling and p53 pathways. Adv Cancer Res. 2018;140:191–215. [PubMed: 30060809]
17. Heffernan-Stroud LA, Obeid LM. p53 and regulation of bioactive sphingolipids. Adv Enzyme Regul. 2011;51:219–228. [PubMed: 21035490]
18. Taha TA, Osta W, Kozhaya L, et al. Down-regulation of sphingosine kinase-1 by DNA damage: dependence on proteases and p53. J Biol Chem. 2004;279:20546–20554. [PubMed: 14988393]
19. Heffernan-Stroud LA, Helke KL, Jenkins RW, De Costa AM, Hannun YA, Obeid LM. Defining a role for sphingosine kinase 1 in p53-dependent tumors. Oncogene. 2012;31:1166–1175. [PubMed: 21765468]
20. Alshaker H, Sauer L, Monteil D, et al. Therapeutic potential of targeting SK1 in human cancers. Adv Cancer Res. 2013;117:143–200. [PubMed: 23290780]

21. Powell JA, Lewis AC, Zhu W, et al. Targeting sphingosine kinase 1 induces MCL1-dependent cell death in acute myeloid leukemia. Blood. 2017;129:771–782. [PubMed: 27956387]
22. Marei HE, Althani A, Afifi N, et al. p53 signaling in cancer progression and therapy. Cancer Cell Int. 2021;21:703. [PubMed: 34952583]
23. Kandoth C, McLellan MD, Vandin F, et al. Mutational landscape and significance across 12 major cancer types. Nature. 2013;502:333–339. [PubMed: 24132290]
24. Xu P, Liu X, Ouyang J, Chen B. TP53 mutation predicts the poor prognosis of non-Hodgkin lymphomas: evidence from a meta-analysis. PLOS One. 2017;12:e0174809. [PubMed: 28369138]
25. Hoshida Y, Hongyo T, Xu JX, et al. TP53 gene mutation, an unfavorable prognostic factor for malignant lymphomas in auto-immune diseases. Oncology. 2005;69:175–183. [PubMed: 16131817]
26. Pappu R, Schwab SR, Cornelissen I, et al. Promotion of lymphocyte egress into blood and lymph by distinct sources of sphingosine-1-phosphate. Science. 2007;316:295–298. [PubMed: 17363629]
27. Espaillat MP, Snider AJ, Qiu Z, et al. Loss of acid ceramidase in myeloid cells suppresses intestinal neutrophil recruitment. FASEB J. 2018;32:2339–2353. [PubMed: 29259036]
28. Bielawski J, Pierce JS, Snider J, Rembiesa B, Szulc ZM, Bielawska A. Comprehensive quantitative analysis of bioactive sphingolipids by high-performance liquid chromatography-tandem mass spectrometry. Methods Mol Biol. 2009;579:443–467. [PubMed: 19763489]
29. Dbaibo GS, Pushkareva MY, Rachid RA, et al. p53-dependent ceramide response to genotoxic stress. J Clin Invest. 1998;102:329–339. [PubMed: 9664074]
30. Jinadasa R, Balmus G, Gerwitz L, Roden J, Weiss R, Duhamel G. Derivation of thymic lymphoma T-cell lines from atm(−/−) and p53(−/−) mice. J Vis Exp. 2011;50:2598.
31. Skordos I, Demeyer A, Beyaert R. Analysis of T cells in mouse lymphoid tissue and blood with flow cytometry. STAR Protoc. 2021;2:100351. [PubMed: 33665631]
32. Tada H, Shiho O, Kuroshima K, Koyama M, Tsukamoto K. An improved colorimetric assay for interleukin 2. J Immunol Methods. 1986;93:157–165. [PubMed: 3490518]
33. Carroll BL, Bonica J, Shamseddine AA, Hannun YA, Obeid LM. A role for caspase-2 in sphingosine kinase 1 proteolysis in response to doxorubicin in breast cancer cells—implications for the CHK1-suppressed pathway. FEBS Open Bio. 2018;8:27–40.
34. Donehower LA, Harvey M, Vogel H, et al. Effects of genetic background on tumorigenesis in p53-deficient mice. Mol Carcinog. 1995;14:16–22. [PubMed: 7546219]
35. Jacks T, Remington L, Williams BO, et al. Tumor spectrum analysis in p53-mutant mice. Curr Biol. 1994;4:1–7. [PubMed: 7922305]
36. Schnute ME, McReynolds MD, Kasten T, et al. Modulation of cellular S1P levels with a novel, potent and specific inhibitor of sphingosine kinase-1. Biochem J. 2012;444:79–88. [PubMed: 22397330]
37. MacRitchie N, Volpert G, Al Washih M, et al. Effect of the sphingosine kinase 1 selective inhibitor, PF-543 on arterial and cardiac remodelling in a hypoxic model of pulmonary arterial hypertension. Cell Signal. 2016;28:946–955. [PubMed: 27063355]
38. Cuvillier O, Nava VE, Murthy SK, et al. Sphingosine generation, cytochrome c release, and activation of caspase-7 in doxorubicin-induced apoptosis of MCF7 breast adenocarcinoma cells. Cell Death Differ. 2001;8:162–171. [PubMed: 11313718]
39. Kuhn R, Schwenk F, Aguet M, Rajewsky K. Inducible gene targeting in mice. Science. 1995;269:1427–1429. [PubMed: 7660125]
40. Allende ML, Sasaki T, Kawai H, et al. Mice deficient in sphingosine kinase 1 are rendered lymphopenic by FTY720. J Biol Chem. 2004;279:52487–52492. [PubMed: 15459201]
41. Breart B, Ramos-Perez WD, Mendoza A, et al. Lipid phosphate phosphatase 3 enables efficient thymic egress. J Exp Med. 2011;208:1267–1278. [PubMed: 21576386]
42. Schwab SR, Pereira JP, Matloubian M, Xu Y, Huang Y, Cyster JG. Lymphocyte sequestration through S1P lyase inhibition and disruption of S1P gradients. Science. 2005;309:1735–1739. [PubMed: 16151014]
43. De la Cueva E, Garcia-Cao I, Herranz M, et al. Tumorigenic activity of p21Waf1/Cip1 in thymic lymphoma. Oncogene. 2006;25:4128–4132. [PubMed: 16462758]

44. Honore B, Vorum H, Pedersen AE, Buus S, Claesson MH. Changes in protein expression in p53 deleted spontaneous thymic lymphomas. Exp Cell Res. 2004;295:91–101. [PubMed: 15051493]
45. Liao MJ, Zhang XX, Hill R, et al. No requirement for V(D)J recombination in p53-deficient thymic lymphoma. Mol Cell Biol. 1998;18:3495–3501. [PubMed: 9584189]
46. Hwang SM, Ha YJ, Koo GB, et al. LCK-mediated RIPK3 activation controls double-positive thymocyte proliferation and restrains thymic lymphoma by regulating the PP2A-ERK Axis. Adv Sci (Weinh). 2022;9:e2204522. [PubMed: 36161785]
47. Date Y, Taniuchi I, Ito K. Oncogenic Runx1-Myc axis in p53-deficient thymic lymphoma. Gene. 2022;819:146234. [PubMed: 35114276]
48. Shakiba N, Jones RD, Weiss R, Del Vecchio D. Context-aware synthetic biology by controller design: engineering the mammalian cell. Cell Syst. 2021;12:561–592. [PubMed: 34139166]
49. Dudgeon C, Chan C, Kang W, et al. The evolution of thymic lymphomas in p53 knockout mice. Genes Dev. 2014;28:2613–2620. [PubMed: 25452272]
50. Xu M, Yu Q, Subrahmanyam R, Difilippantonio MJ, Ried T, Sen JM. Beta-catenin expression results in p53-independent DNA damage and oncogene-induced senescence in prelymphomagenic thymocytes in vivo. Mol Cell Biol. 2008;28:1713–1723. [PubMed: 18160717]
51. Nava VE, Cuvillier O, Edsall LC, et al. Sphingosine enhances apoptosis of radiation-resistant prostate cancer cells. Cancer Res. 2000;60:4468–4474. [PubMed: 10969794]
52. Ahn EH, Lee MB, Seo DJ, Lee J, Kim Y, Gupta K. Sphingosine induces apoptosis and Down-regulation of MYCN in PAX3-FOXO1-positive alveolar rhabdomyosarcoma cells irrespective of TP53 mutation. Anticancer Res. 2018;38:71–76. [PubMed: 29277758]
53. Bode C, Berlin M, Rostel F, Teichmann B, Graler MH. Evaluating sphingosine and its analogues as potential alternatives for aggressive lymphoma treatment. Cell Physiol Biochem. 2014;34:1686–1700. [PubMed: 25401781]
54. Cuvillier O, Edsall L, Spiegel S. Involvement of sphingosine in mitochondria-dependent Fas-induced apoptosis of type II Jurkat T cells. J Biol Chem. 2000;275:15691–15700. [PubMed: 10747891]
55. Woodcock J Sphingosine and ceramide signalling in apoptosis. IUBMB Life. 2006;58:462–466. [PubMed: 16916783]
56. Nganga R, Oleinik N, Ogretmen B. Mechanisms of ceramide-dependent cancer cell death. Adv Cancer Res. 2018;140:1–25. [PubMed: 30060806]
57. Li MH, Hla T, Ferrer F. FTY720 inhibits tumor growth and enhances the tumor-suppressive effect of topotecan in neuroblastoma by interfering with the sphingolipid signaling pathway. Pediatr Blood Cancer. 2013;60:1418–1423. [PubMed: 23704073]
58. Jozefczuk E, Nosalski R, Saju B, et al. Cardiovascular effects of pharmacological targeting of sphingosine kinase 1. Hypertension. 2020;75:383–392. [PubMed: 31838904]
59. Liu J, Jiang B. Sphk1 promotes ulcerative colitis via activating JAK2/STAT3 signaling pathway. Hum Cell. 2020;33:57–66. [PubMed: 31606874]
60. Wang C, Xu T, Lachance BB, et al. Critical roles of sphingosine kinase 1 in the regulation of neuroinflammation and neuronal injury after spinal cord injury. J Neuroinflammation. 2021;18:50. [PubMed: 33602274]
61. Ha AW, Sudhadevi T, Ebenezer DL, et al. Neonatal therapy with PF543, a sphingosine kinase 1 inhibitor, ameliorates hyperoxia-induced airway remodeling in a murine model of bronchopulmonary dysplasia. Am J Physiol Lung Cell Mol Physiol. 2020;319:L497–L512. [PubMed: 32697651]
62. Du C, Ren Y, Yao F, et al. Sphingosine kinase 1 protects renal tubular epithelial cells from renal fibrosis via induction of autophagy. Int J Biochem Cell Biol. 2017;90:17–28. [PubMed: 28733250]
63. Kim SB, Limbu KR, Oh YS, et al. Novel dimer derivatives of PF-543 as potential antitumor agents for the treatment of non-small cell lung cancer. Pharmaceutics. 2022;14(10):2035 [PubMed: 36297469]
64. Shamshiddinova M, Gulyamov S, Kim HJ, Jung SH, Baek DJ, Lee YM. A Dansyl-modified sphingosine kinase inhibitor DPF-543 enhanced De novo ceramide generation. Int J Mol Sci. 2021;22:9190. [PubMed: 34502095]

65. Riboni L, Abdel Hadi L, Navone SE, Guarnaccia L, Campanella R, Marfia G. Sphingosine-1-phosphate in the tumor microenvironment: a signaling hub regulating cancer hallmarks. Cell. 2020;9:337–370.

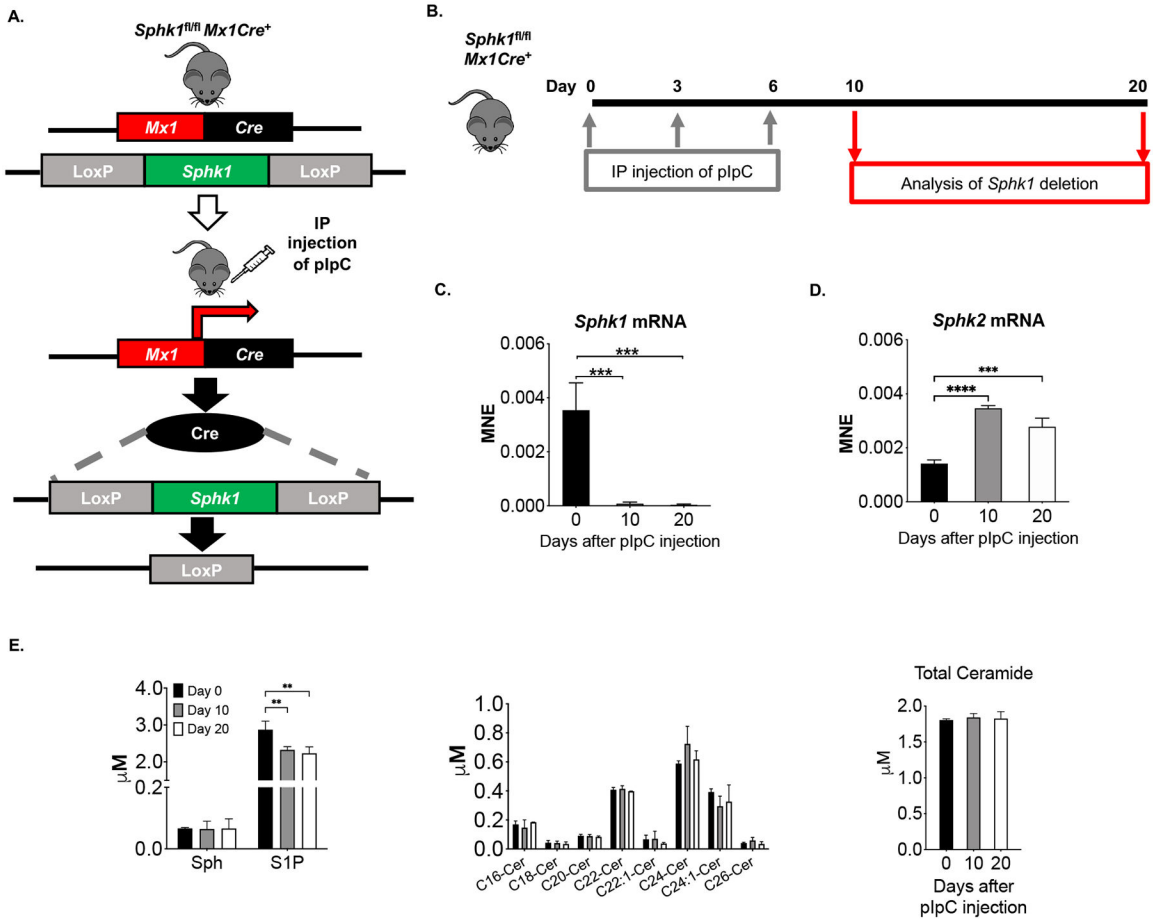

FIGURE 1.

Efficient deletion of *Sphk1* in the thymus of *Sphk1*$^{fl/fl}$ *Mx1Cre*$^{+}$ mice. (A) Scheme illustrating the induction of Cre expression and subsequent recombination after IP injection of pIpC in *Sphk1*$^{fl/fl}$ *Mx1Cre*$^{+}$ mice. (B) Protocol used to induce *Sphk1* deletion in the thymus of *Sphk1*$^{fl/fl}$ *Mx1Cre*$^{+}$ mice. (C) and (D) *Sphk1*$^{fl/fl}$ *Mx1Cre*$^{+}$ mice were injected 3 times with pIpC (protocol shown in B). *Sphk1* (C) and *Sphk2* (D) mRNA expression were analyzed by qPCR at day 0, 10 and 20 after the first injection. Statistical analysis: one-way ANOVA, Dunnett's multiple comparison test, ***$p < .0005$. (E) Sphingolipid levels were measured in blood by LC/MS at day 0, 10 and 20 after the first injection with pIpC (protocol shown in Figure B). Two independent samples were analyzed per each point. Statistical analysis: 2-way ANOVA, Sidak's multiple comparison test, **$p < .001$.

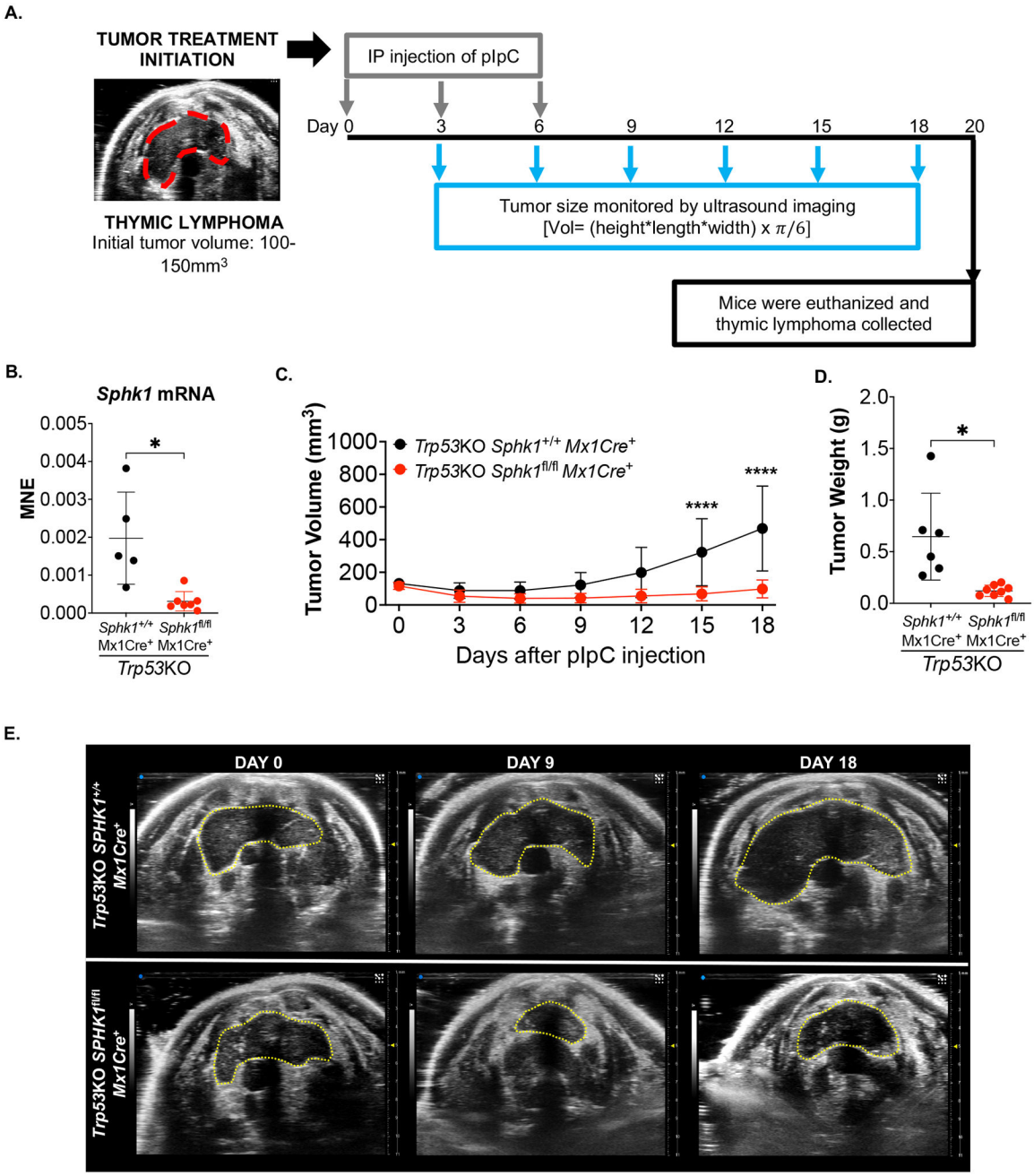

FIGURE 2.

Sphk1 ablation in *Trp53*KO mice abates thymic lymphoma progression. (A) Protocol used in *Trp53*KO *Sphk1*$^{fl/fl}$ *Mx1Cre*$^{+}$ mice to delete *Sphk1* once thymic lymphoma was detected by ultrasound imaging. (B) *Sphk1* mRNA *mRNA* expression was analyzed by qPCR in thymic lymphoma from *Trp53*KO *Sphk1*$^{+/+}$ *Mx1Cre*$^{+}$ (control) and *Trp53*KO *Sphk1*$^{fl/fl}$ *Mx1Cre*$^{+}$ mice at day 20 after tumor treatment initiation. Statistical analysis: Unpaired *t* test with Welch's correction for *Trp53*KO vs *Trp53*KO *Sphk1*$^{fl/fl}$ *Mx1Cre*$^{+}$, $*p < .005$. (C) Tumor size for thymic lymphoma from *Trp53*KO *Sphk1*$^{+/+}$ *Mx1Cre*$^{+}$ (control, black, $n = 6$) and *Trp53*KO *Sphk1*$^{fl/fl}$ *Mx1Cre*$^{+}$ (red, $n = 8$) mice treated in accordance to protocol shown in

Figure 2A. Statistical analysis: 2-way ANOVA, Sidak's multiple comparison test, ***$p <$ .0005; ****$p <$ .0001. (D) Analysis of tumor weight at day 20 after treatment initiation in *Trp53*KO *Sphk1*$^{+/+}$ *Mx1Cre*$^{+}$ (control, black, $n = 6$) and *Trp53*KO *Sphk1*$^{fl/fl}$ *Mx1Cre*$^{+}$ (red, $n = 8$) mice. Unpaired *t* test with Welch's correction for *Trp53*KO vs *Trp53*KO *Sphk1*$^{fl/fl}$ *Mx1Cre*$^{+}$, *$p <$ .005. (E) Representative examples of coronal ultrasound images of thymic lymphomas in *Trp53*KO *Sphk1*$^{+/+}$ *Mx1Cre*$^{+}$ (control) and *Trp53*KO *Sphk1*$^{fl/fl}$ *Mx1Cre*$^{+}$ at day 0, 9 and 18 after tumor treatment initiation.

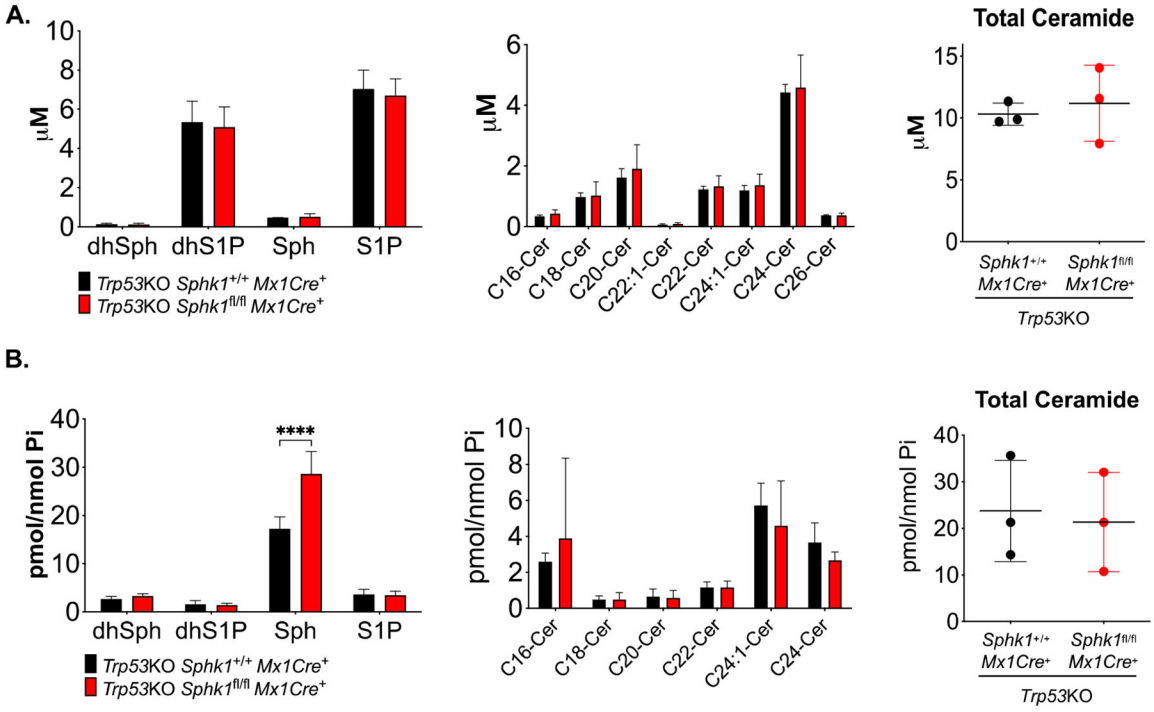

FIGURE 3.

Sphk1 ablation results in selective increase in levels of Sph in *Trp53*KO thymic lymphoma. Thymic lymphoma tissue (A) and blood samples (B) from *Trp53*KO *Sphk1*$^{+/+}$ *Mx1Cre*$^{+}$ (control) and *Trp53*KO *Sphk1*$^{fl/fl}$ *Mx1Cre*$^{+}$ mice at day 20 after tumor treatment initiation were processed for sphingolipid analysis by LC MS/MS. Values shown are the mean ± SD (n = 3). Statistical analysis: 2-way ANOVA, Sidak's multiple comparison test, ***p < .0005.

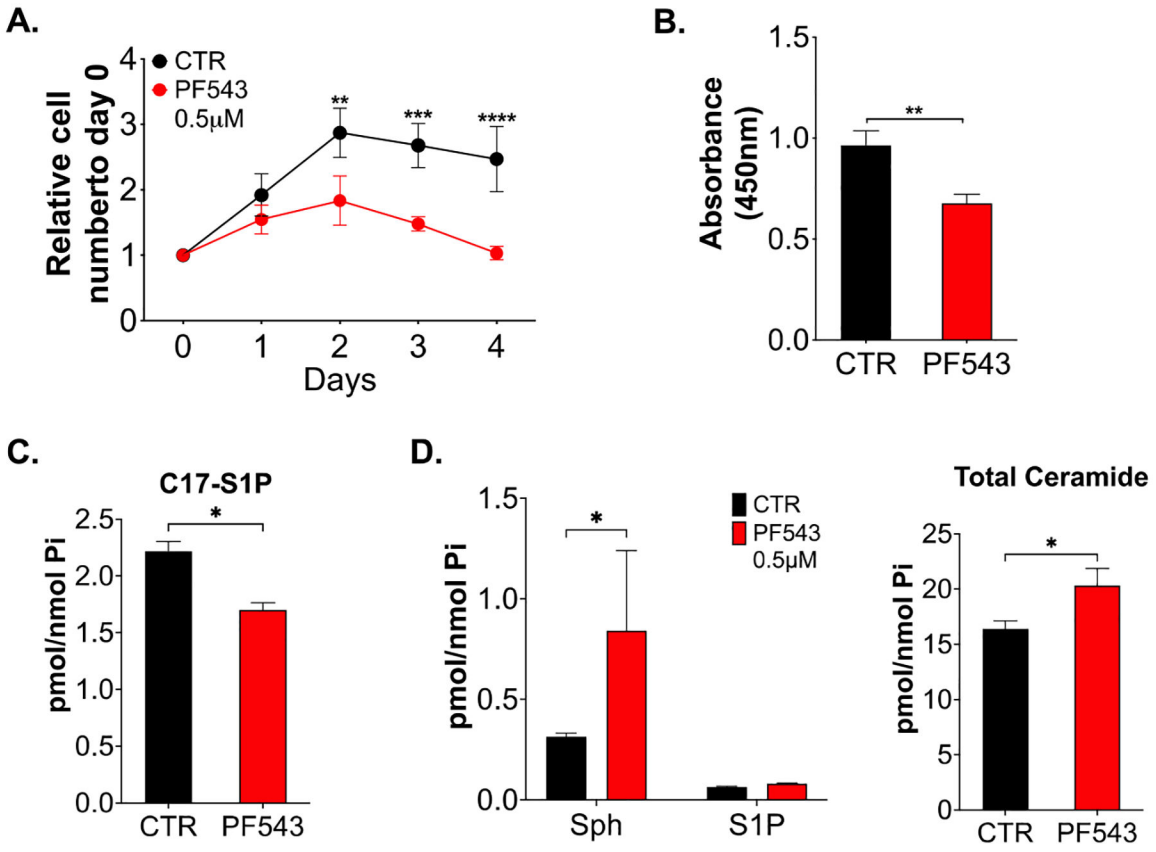

FIGURE 4.

SK1 inhibition decreases cell survival in mouse p53KO thymic lymphoma cells. (A) Mouse p53KO thymic lymphoma cells were treated with vehicle (black line) or PF543 0.5 μM (red line) and cells were counted by trypan blue exclusion every day for 4 days. Data shown are mean ± SD ($n = 4$). Statistical analysis: 2-way ANOVA $^{**}p < .001$; $^{***}p < .0005$; $^{****}p < .0001$. (B) Cell viability was measured by CCK-8 assay at day 2 after treatment with vehicle (control, black bar) or PF543 0.5 μM (red bar). Data shown are mean ± SD ($n = 4$). Statistical analysis: Unpaired *t* test with Welch's correction $^{**}p < .001$. (C) Sphingosine kinase activity was measured after 24 h of treatment with vehicle (control, black bar) or PF543 0.5 μM (red bar). C17-Sphingosine was added to the cells 20 min before cell collection, and after lipid extraction C17-S1P was measured by LC/MS. Data shown are mean ± SD ($n = 2$). Statistical analysis: Unpaired *t* test with Welch's correction $^{*}p < .005$. (D) Mouse p53KO thymic lymphoma cells treated with vehicle (black line) or PF543 0.5 μM (red line) were processed for sphingolipid analysis by LC MS/MS. Values shown are the mean ± SD ($n = 2$). Statistical analysis for Sph and S1P: 2-way ANOVA, Sidak's multiple comparison test, $^{*}p < .05$. Statistical analysis: Unpaired *t* test with Welch's correction $^{*}p < .005$. Statistical analysis for total ceramide: Unpaired *t* test with Welch's correction $^{*}p < .005$.

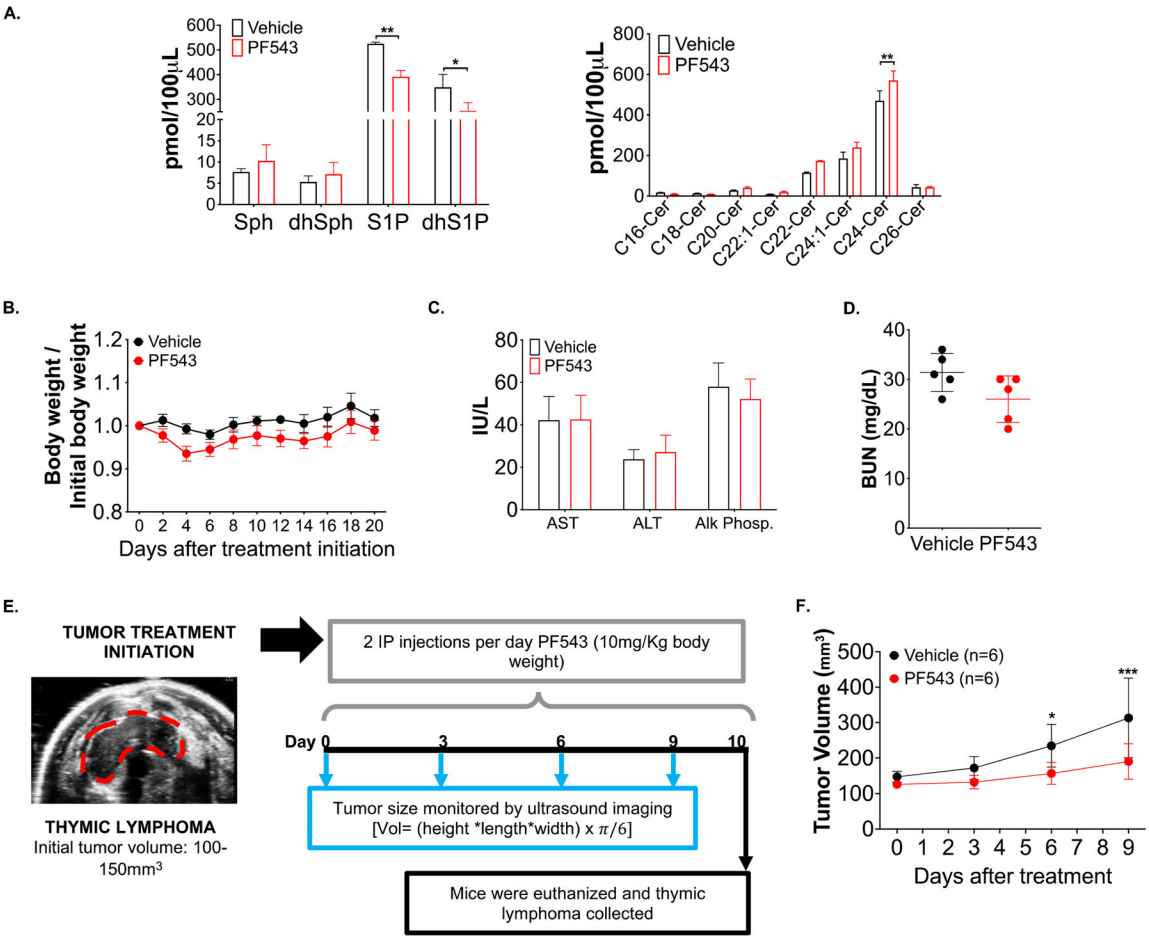

FIGURE 5.

Pharmacological inhibition of SK1 controls thymic lymphoma growth in *Trp53*KO mice. (A) Blood samples from mice treated with vehicle (black bar) or PF543 (red bar, 10 mg/kg of body weight) after 2 h of IP injection were processed for sphingolipid analysis by LC MS/MS. Values shown are the mean ± SD ($n = 2$). Statistical analysis: 2-way ANOVA, Sidak's multiple comparison test, *$p < .005$; **$p < .001$. (B) Body weight was assessed every two days in mice treated with vehicle (black line) or PF543 (red line, 10 mg/kg of body weight) with 2 IP injections per day for 20 days. (C) Concentration of liver enzymes was evaluated in blood samples from mice treated with Vehicle (black bar) or PF543 (red bar, 10 mg/kg of body weight) with 2 IP injections per day for 20 days. (D) Blood Urea Nitrogen (BUN) was measured in mice treated with Vehicle (black bar) or PF543 (red bar, 10 mg/kg of body weight) with 2 IP injections per day for 20 days. (E) Blood counts were performed on whole blood from mice treated with vehicle (black circle, $n = 5$) or PF543 (red circle, 10 mg/kg of body weight, $n = 5$) with 2 IP injections per day for 20 days. Blood was analyzed for lymphocytes and white blood cells (WBCs) number. (F) Protocol of treatment with PF543 in *Trp53*KO mice once thymic lymphoma was detected by ultrasound imaging. (G) Tumor size of thymic lymphoma from *Trp53*KO mice treated with vehicle (control, black, $n = 6$) or PF543 (red, $n = 6$) accordance to protocol shown in Figure 5E. Statistical analysis: 2-way ANOVA, Sidak's multiple comparison test, *$p < .005$; ***$p < .0005$.

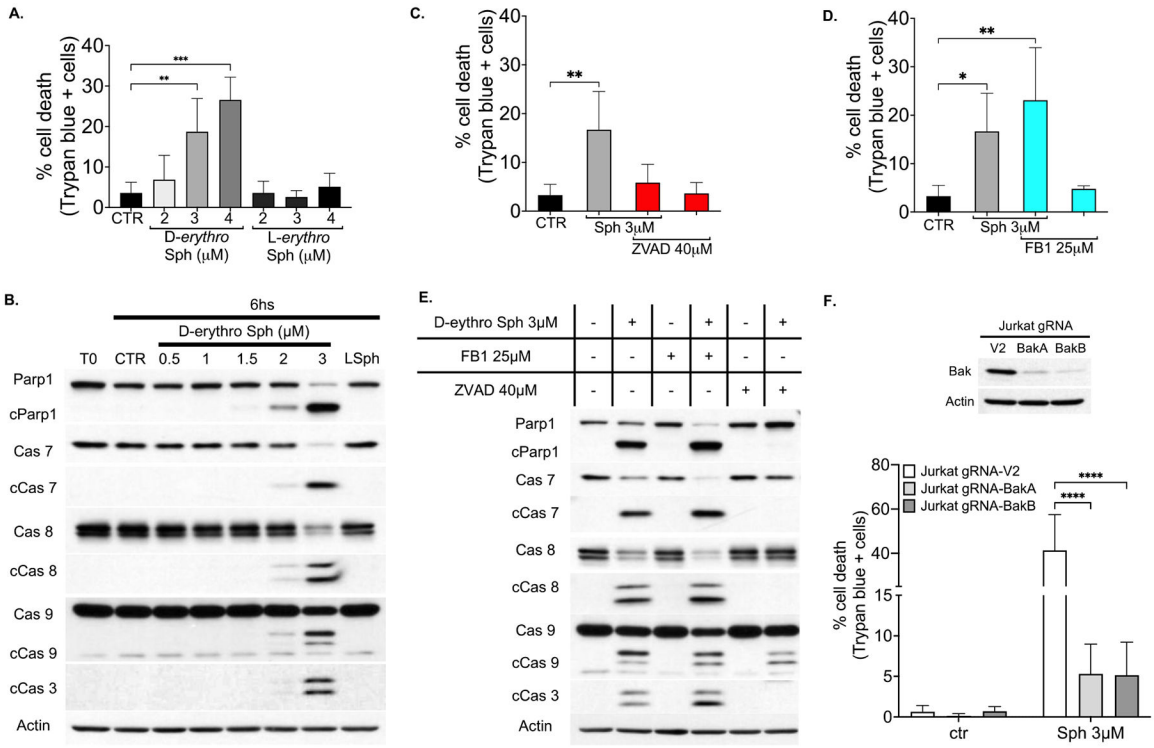

FIGURE 6.

Sph induces cell death in Molt4E6 cells. (A) Histogram representing the percentage of cell death for Molt4E6 cells treated with vehicle, D-erythro-Sph or L-erythro-Sph. Cells were counted by trypan blue exclusion after 24 h of treatment. Data shown are mean ± SD ($n = 3$). Statistical analysis: one-way ANOVA, Dunnett's multiple comparison test, ***$p < .0005$, **$p < .001$. (B) Molt4E6 cells were treated with different concentrations of D-eryhtro-Sph, and protein samples were analyzed by Western blot after 6 h of treatment. Specific antibodies against each protein were used as probes. Actin served as internal loading control. (C) Molt4 E6 cells were pre-treated with ZVAD 40 μM for 1 h and then treated with 3 μM of D-erythro-Sph. 24 h after treatment, cells were counted by trypan blue exclusion. Data shown are mean ± SD ($n = 4$). Statistical analysis: one-way ANOVA, Dunnett's multiple comparison test, **$p < .001$. (D) Molt4 E6 cells were pre-treated with FB1 25 μM for 1 h and then treated with 3 μM of D-erythro-Sph. 24 h after treatment, cells were counted by trypan blue exclusion. Data shown are mean ± SD ($n = 4$). Statistical analysis: one-way ANOVA, Dunnett's multiple comparison test, **$p < .001$, *$p < .005$. (E). Molt4E6 cells were pre-treated with FB1 25 μM or ZVAD 40 μM for 1 h and then treated with 3 μM of D-eryhtro-Sph. 6 h after Sph addition, samples were collected and protein analyzed by Western blot. Specific antibodies against each protein were used as probes. Actin served as internal loading control. (F) Percentage of cell death for Jurkat sgRNA V2 (control cells), Jurkat sgRNA BakA and Jurkat sgRNA BakB cells treated with vehicle or D-erythro-Sph. Cells were counted by trypan blue exclusion after 24 h of treatment. Data shown are mean ± SD ($n = 3$). Statistical analysis: 2-way ANOVA, Sidak's multiple comparison test, ****$p < .0001$. Upper Western blot showed the decreased Bak expression in Jurkat cells after transduction.

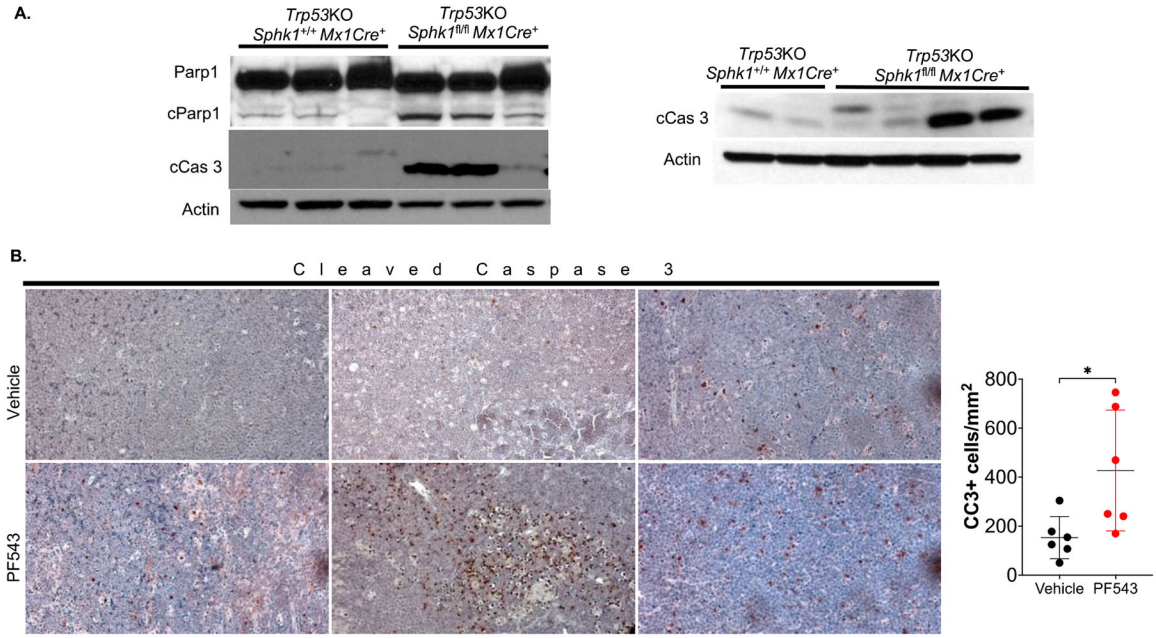

FIGURE 7.

Targeting SK1 in *Trp53*KO mice controls thymic lymphoma growth by increased apoptosis. (A) Western blot analysis for cleaved caspase 3 and Parp1 protein expression in lymphoma tissue samples from *Trp53*KO *Sphk1*$^{+/+}$ *Mx1Cre*$^{+}$ (control) and *Trp53*KO *Sphk1*$^{fl/fl}$ *Mx1Cre*$^{+}$ mice at day 20 after initiation of treatment. Actin served as internal loading control. (B) Immunohistochemistry staining for cleaved caspase 3 of tumor tissue sections dissected from *Trp53*KO mice treated with vehicle or PF543 at day 10 after tumor treatment initiation. Representative images from three mice per each condition are shown. Quantification of the number of cleaved caspase 3 positive cells per mm^2 is shown on the right. Statistical analysis: Unpaired *t* test with Welch's correction *$p < .005$.

TABLE 1

Pharmacokinetics of PF543 in wildtype mice.

25mg/Kg

Subject	$T_{1/2}$	T_{max}	C_{max}	C_{max}	AUC_{last}	AUC_{last}	AUC_{INF_obs}	AUC	Cl_obs
	hr	*hr*	*ng/mL*	*μM*	*min*ng/mL*	*μM.hr*	*min*ng/mL*	*%Extrap*	*mL/min/kg*
Mouse-1	4.81	0.25	1490	3.20	106790	3.82	107747	0.89	232.02
Mouse-2	4.88	0.25	879	1.89	74364	2.66	75251	1.18	332.22
Mouse-3	4.35	0.25	1690	3.63	110076	3.94	110791	0.65	225.65
Avg.	**4.68**	**0.25**	**1353**	**2.91**	**97077**	**3.47**	**97930**	**0.90**	**263.30**

50mg/Kg

Subject	$T_{1/2}$	T_{max}	C_{max}	C_{max}	AUC_{last}	AUC_{last}	AUC_{INF_obs}	AUC	Cl_obs
	hr	*hr*	*ng/mL*	*μM*	*min*ng/mL*	*μM.hr*	*min*ng/mL*	*%Extrap*	*mL/min/kg*
Mouse-4	3.91	0.25	382	0.82	61908	2.22	62552	1.03	799.34
Mouse-5	3.62	0.25	2710	5.82	279045	9.99	280080	0.37	178.52
Mouse-6	5.04	0.25	2950	6.34	374931	13.42	379644	1.24	131.70
Avg.	**4.19**	**0.25**	**2014**	**4.33**	**238628**	**8.54**	**240758**	**0.88**	**369.85**

100mg/Kg[*]

Subject	$T_{1/2}$	T_{max}	C_{max}	C_{max}	AUC_{last}	AUC_{last}	AUC_{INF_obs}	AUC	Cl_obs
	hr	*hr*	*ng/mL*	*μM*	*min*ng/mL*	*μM.hr*	*min*ng/mL*	*%Extrap*	*mL/min/kg*
Mouse-7									
Mouse-8	4.19	1.00	4470	9.60	1105425	39.57	1124656	1.71	88.92
Mouse-9	8.24	0.50	4950	10.63	793731	28.41	828751	4.23	120.66
Avg.	**6.22**	**0.75**	**4710**	**10.12**	**949578**	**33.99**	**976704**	**2.97**	**104.79**

[*]#7,8,9 were severe lethargic. #7 had seizures and died at 30min. #8&9 slowly recovered.